Observational Study

Medicine

OPEN

Examination of the microstructures of the lower cervical facet based on micro-computed tomography

A cadaver study

Kun Li, MD[a,b], Yucheng Ji, MD[b], Jun Shi, PhD[c], Shaojie Zhang, PhD[b], Haoyu Song, MSc[c], Peng Wang, MSc[c], Chunying Ma, MSc[c], Yansong Zhang, MSc[c], Yexing Dang, MSc[c], Yuan Ma, MSc[c], Xing Wang, PhD[a,b], Zhijun Li, PhD[a,b,*]

Abstract

The cervical facet has complicated 3D microstructures and inhomogeneities. The cervical facet joint, which also participates in the formation, plays a certain role in regulating and limiting the movement of the spine. Correct identification and evaluation of its microstructure can help in the diagnosis of orthopedic disease and predict early phases of fracture risk. To evaluate the safety of the cervical spine by measuring and analyzing the microstructures and morphometric parameters of bone trabeculae in the normal cervical facet with high-resolution 3D micro-computed tomography. Thirty-one sets of C3 to C7 lower cervical vertebrae (155 vertebrae) were scanned using micro-computed tomography. The morphological characteristics and direction of trabecular bone in the facet of the lower cervical vertebrae were observed by selecting and rebuilding the areas of interest, and the changes in the microstructure of the areas of interest were calculated to reveal the structural characteristics and weak areas. Images indicated an ossified center between the superior and inferior articular processes of the lower cervical spine. The cellular bone trabeculae of the articular process had complex reticular microstructures. The trabecular bone plate near the cortical bone was lamellar and relatively dense, and it extended around and transformed into a network structure, and then into the rod-shaped trabecular bone. The rod-shaped trabeculae converged with the plate-shaped trabeculae with only 1 to 2 layers surrounding the trabeculae cavity. Statistical results of the morphological parameters of the trabecular bone showed that trabecular bone volume fraction values were significantly higher for C7 than for C3 to C6 ($P < .05$). There were significant differences between C7 and C3 to C5 and between C6 and C4 in bone surface area/bone volume ($P < .05$). There was a significant difference between C7 and C3 to C6 in trabecular bone thickness values ($P < .05$). The degree of anisotropy value was significantly smaller for C3 than for C6 and C7 ($P < .05$). The changes in the C3 to C7 microstructure were summarized in this study. The loading capacity and stress of the C7 articular process tended to be limited, and the risk of injury tended to be higher for the C7 articular process.

Abbreviations: BS/TB = bone surface density, BV/TV = bone surface area/bone volume, micro-CT = micro-computed tomography, ROI = region of interest, Tb.n = trabecular number, Tb.Pf = trabecular pattern factor, Tb.Sp = trabecular space, Tb.Th = trabecular bone thickness.

Keywords: cervical spine, facet joint, micro-computed tomography, microstructure, trabecular bone

The authors received funding from the National Natural Science Foundation of China (grant numbers 81860382 and 81860383); Inner Mongolia Natural Science Foundation (grant numbers 2022QN03002, 2020MS03061, 2019MS08117, and 2019MS08139); Inner Mongolia Autonomous Region Science and Technology Development Plan Project (grant number 2019GG158). Supported By Program for Young Talents of Science and Technology in Universities of Inner Mongolia Autonomous Region (grant number NJYT22009); Key Scientific Research projects of Inner Mongolia Medical University (grant number YKD2021ZD011); Medical and Health Science and Technology Plan Project of Health Commission of Inner Mongolia Autonomous region (grant number 202201217); Youth Fund Project of Inner Mongolia Medical University (grant number YKD2020QNCX055); Student Innovation and Entrepreneurship Project of Inner Mongolia Medical University (grant number 202210132011, 202210132031).

The authors have no conflicts of interest to disclose.

The datasets generated during and/or analyzed during the current study are available from the corresponding author on reasonable request.

[a] Beijing University of Chinese Medicine School of Traditional Chinese Medicine, Beijing, China, [b] Human Anatomy Teaching and Research Section (Digital Medical Center), Inner Mongolia Medical University Basic Medical College, Hohhot, China, [c] Department of Physiology, School of Basic Medicine, Inner Mongolia Medical University, Hohhot, China.

**Correspondence: Zhijun Li and Xing Wang, Beijing University of Chinese Medicine School of Traditional Chinese Medicine, Yangguang South Street, Fangshan District, Beijing 100029, China (e-mail: 13904717040@qq.com and wangxing197911@163.com).*

How to cite this article: Li K, Ji Y, Shi J, Zhang S, Song H, Wang P, Ma C, Zhang Y, Dang Y, Ma Y, Wang X, Li Z. Examination of the microstructures of the lower cervical facet based on micro-computed tomography: A cadaver study. Medicine 2022;101:50(e31805).

Received: 26 August 2022 / Received in final form: 23 October 2022 / Accepted: 25 October 2022

http://dx.doi.org/10.1097/MD.0000000000031805

1. Introduction

The cervical facet is an important structure involved in spinal movement, and its fracture or injury often causes loss of spinal stability and spinal nerve injury, which is an important cause of cervical diseases.[1–3] However, due to the complex anatomical structure of the lower cervical spine, treatment can be challenging. Most conventional computed tomography (CT) examinations can detect cervical facet injuries or fractures at an early stage, but conventional images are obtained with low-resolution imaging methods and the detection level is insufficient for microstructural analysis. Osteoporosis is a systemic metabolic bone disease that is characterized by decreased bone mineral density and changes in trabecular bone structure and number, resulting in increased bone fragility and easy fracture. Bone mineral density measurement is one of the "gold standards" for diagnosis. At present, radiography, CT, and magnetic resonance imaging cannot clearly reveal the internal microstructure of bone.[4] Micro-CT is a nondestructive and high-resolution imaging method that can display the microstructure of bone specimens and accurately distinguish trabecular bone from cortical bone. High-resolution scanning, which can be used to clearly observe the bone cortex and trabecular bone configuration and morphological characteristics, has become the current "gold standard" tool for evaluating bone shape, bone microstructure, and the articular process within the trabecular bone. Spatial resolution in the micron range, for 3D imaging equipment, has been applied in the analysis of bone structure; the resolution is 100 times higher than that of conventional CT,[5–8] and it provides a theoretical basis for the diagnosis, treatment, and prevention of diseases. However, there are few studies on the use of micro-computed tomography (micro-CT) for determining the microstructure parameters of the articular process, the morphology of bone trabeculae, and the prediction of pathogenicity.

This study utilized micro-CT to study the lower cervical facet and evaluate its 3D microstructure by analyzing morphological characteristics. Analysis software was used to analyze the trabecular bone parameters in the selected area of interest and describe the structural characteristics of trabecular bone, with a view to providing diagnosis and treatment strategies for facet disease.

2. Methods

2.1. Designates

Micro-CT was used to analyze the trabecular shape of the articular process of the lower cervical spine and to measure the bone microstructure.

2.2. Time and places

The experiment was completed in the Digital Medical Center of a Grade III Level A hospital in China from July to October 2021.

2.3. Materials

This study was conducted with Chinese human dried bone specimens from the Anatomy Laboratory of Inner Mongolia Medical University. In accordance with the requirements of bone anthropology identification standards, 31 sets of normal lower cervical vertebra bone specimens were selected from dry adult bones, with 310 articular processes in total. Bone specimens with bone damage and defects were excluded. This study was approved by the Medical Ethics Committee of Inner Mongolia Medical University (Approval Number: YKD2018031). This study was exempt from the requirement for informed consent because the research used cadavers.

2.4. Imaging

Micro-CT was performed using a micro-CT scanner (Inveon PET/CT; Siemens, Erlangen, Germany) with complete C3 to C7 in the scanning slot. The scanning parameters were source voltage 80 kVp, current 500 μA, and exposure time 600 ms. Each specimen was scanned continuously with a layer thickness of 1 pixel and a layer spacing of 1 pixel. The Micro-CT software (Inveon Research Workplace software, multi-mode 3D visualization; Siemens) stored the image scans in CTA format.

2.5. Observations and measurements

The original DICOM data from continuous micro-CT scanning were imported into the main interface of the Inveon Research Workplace without damage and compression. Coronal, horizontal, and sagittal 2D images were displayed by entering the main interface and selecting "General Analysis," and the microscopic morphology of specimens was displayed for parallel analysis and description. Multimodal 3D visualization was selected to display coronal, horizontal, and sagittal 2D images and 3D reconstructed images of the specimens. The selection was carried out in the XZ plane, and the regions of interest (ROIs) were manually selected from the trabecular bone and bone marrow plane images with threshold binarization in the horizontal 2D image (ROI was outlined from the processed image forms including cuboids, circles, ellipses, and irregular polygons). The trabecular bone volume fraction (BV/TV, %), bone surface area/bone volume (BS/BV, mm^{-1}), trabecular bone thickness (Tb.Th, mm), bone surface density (BS/TB, mm^{-1}), trabecular number (Tb.n, mm^{-1}), trabecular space (Tb.Sp, mm), degree of anisotropy, and trabecular pattern factor (Tb.Pf, mm^{-1}) were calculated (Table 1).

2.6. Statistical analysis

The measured data were input into Excel (Microsoft Corp., Redmond, WA) and analyzed with IBM SPSS version 21.0 statistical software (IBM Corp., Armonk, NY). All values are expressed as mean ± standard deviation (X 12 ± S). The measurement data were tested for normal distribution. A paired *t* test was utilized to compare the left and right dimensions, and

Table 1

Description and definition of cancellous bone 3D results.

Variables	Definitions
Bone volume/total volume (BV/TV)	Ratio of bone trabecular volume to interzone volume
Bone surface/total volume (BS/BV, mm^{-1})	Ratio of bone surface area to total volume in fields of interest
Bone surface density (BS/TB, mm^{-1})	Ratio of bone surface area to total volume in fields of interest
Trabecular thickness (Tb.Th, mm)	Mean thickness of bone trabecular was measured directly with 3D method
Trabecular number (Tb.N, mm^{-1})	Average number of trabeculae per unit length
Trabecular separation (Tb.Sp, mm)	Mean distance between bone trabeculae was measured directly with the 3D method
Degree of anisotropy (DA)	1: isotropy, >1: non-isotropy; DA: equal to the longest intercept length divided by the shortest intercept length
Trabecular bone pattern factor (Tb.Pf, mm^{-1})	The smaller the bone trabecular connectivity, the better the bone trabecular connectivity

one-way analysis of variance was used to compare the intervertebral order. A test level of a = 0.05 was established, and $P < .05$ indicated a statistically significant difference.

3. Results

3.1. Observation of the microstructure and morphology of the articular process

The micro-CT image showed that the bone trabecular cavity formed in the ossification center between the upper and lower articular processes. The microstructure was obviously different from the normal bone trabecular structure. Micro-CT also revealed the complex reticular microstructures of the honeycomb bone trabeculae in the articular processes of the lower cervical spine. The trabecular bone plate near the cortical bone was lamellar and relatively dense, and extended around and transformed into a network structure and then into the rod-shaped trabecular bone. The rod-shaped trabeculae were converged with the plate-shaped trabeculae with only 1 to 2 layers around the trabecular cavity (Fig. 1).

3.2. Trend of the microstructural indexes of the articular processes

The variation trend and regularity of eight groups of microstructural indicators in the C3 to C7 ROI were analyzed (Table 1). There were no significant differences for any indexes on the left and right sides; thus, combined statistics were analyzed. In the intervertebral sequence comparison, the trend of trabecular volume fraction "peaked," with the peak value at C4 and the minimum value at C7, and there was a significant difference between the values of C7 and C3 to C6 ($P < .05$). The trabecular volume fraction was positively correlated with bone hardness, indicating that the bone in C7 was relatively osteoporotic. The shape of the bone surface density was "W-shaped" and located at C7. The bone surface area/bone volume ratio had its peak at C7 which was significantly higher than values for C3, C4, and C5 ($P < .05$). There was also a significant difference between C6 and C4 values ($P < .05$). The opposite trend was generally observed for the trabecular bone volume fraction because when the trabecular bone had a constant surface area and trabecular bone volume, the greater the bone trabecular bone area bone volume, the smaller the volume fraction. This is consistent with the variation law of experimental microstructure parameters. The overall trend of trabecular number, trabecular space, and trabecular thickness was relatively flat, but there were significant differences between C7 and C3 to C6 in trabecular thickness ($P < .05$), while there were no significant differences in other trabecular thicknesses ($P > .05$). There was an increasing trend in the degree of anisotropy, and there was no significant difference between C3 and C6 and C7 ($P < .05$) ($P > .05$). The trabecular bone structure factor was "W-shaped," with the minimum and maximum values located at C4 and C7, respectively; however, there was no significant difference among all the groups ($P > .05$) (Table 2).

4. Discussion

The facet joint, uncinate joint, and intervertebral disc work together to support neck movement. Denis proposed the three-column theory of the spine, in which the posterior column

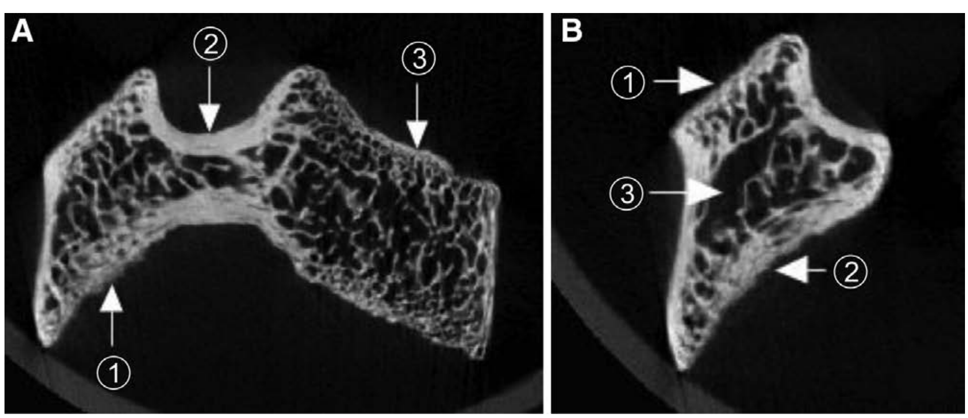

Figure 1. Articular trabecular bone and trabecular cavity (sagittal view). (A) ① articular process; ② vertebral arch pedicle; ③ centrum. (B) ① superior articular process; ② inferior articular process; ③ trabecular cavity.

Table 2

Measurement results of C3–C7 facet joint indexes.

	C3	C4	C5	C6	C7
BV/TV	0.18 ± 0.05*	0.19 ± 0.06*	0.18 ± 0.04*	0.17 ± 0.05*	0.16 ± 0.06
BS/BV	674.92 ± 850.83*	575.62 ± 679.94*,†	698.32 ± 823.17*	952.84 ± 901.34	1014.94 ± 128.90
BS/TB	113.29 ± 161.94	106.59 ± 130.42	123.42 ± 155.91	155.55 ± 147.39	157.13 ± 145.86
Tb.Th	0.13 ± 0.00*	0.13 ± 0.00*	0.13 ± 0.00*	0.13 ± 0.00*	0.13 ± 0.00
Tb.N	3.63 ± 0.13	3.61 ± 0.18	3.64 ± 0.12	3.62 ± 0.14	3.63 ± 0.17
Tb.Sp	3.63 ± 0.13	3.61 ± 0.18	3.64 ± 0.12	3.63 ± 0.14	3.63 ± 0.17
DA	0.30 ± 0.10*,†	0.32 ± 0.10	0.31 ± 0.08	0.34 ± 0.11	0.34 ± 0.13
Tb.Pf	16.48 ± 4.34	16.03 ± 4.52	16.11 ± 3.90	16.29 ± 4.27	17.31 ± 4.91

BS/BV = bone surface area/bone volume, BS/TB = bone surface density, BV/TV = trabecular bone volume fraction, DA = degree of anisotropy, Tb.n = trabecular number, Tb.Pf = trabecular pattern factor, Tb.Sp = trabecular space, Tb.Th = trabecular bone thickness.

*Versus C7.

†Versus C6 ($P < .05$).

bears 20% of the neck motion load. As the main stress structure of the posterior column, the articular process plays an important role in maintaining the stability of the cervical spine and transferring load,[9,10] and its injury or abnormal function causes serious clinical symptoms. Studies on the microstructure of bone trabeculae inside the articular process have the potential to lay the biomechanical foundation for the treatment of cervical spine injuries.

There are three ossification centers in the development of vertebrae, among which the upper and lower ossification centers located in the lateral mass correspond to the upper and lower articular processes. Ossification and fusion occur in ossification centers with increasing age, but aspects such as the specific degree of fusion, whether the fusion is complete, or whether there is a cavity in the middle, have not been reported in specific studies. In this study, micro-CT was used to observe the formation of the bone trabecular cavity in the ossification center between the upper and lower articular processes. We found that the trabecular cavity is formed because the trabecular bone around the ossification center is not completely fused, and the normal trabecular bone structure is filled with trabecular bone. As such, the microstructure is obviously different from the normal trabecular bone structure; therefore, this was an important mechanism in the occurrence of articular process fracture. At the same time, micro-CT can clearly show the complex network microstructure of the honeycomb bone trabecula in the articular process of the lower cervical spine. The trabecular bone plate near the cortical bone was lamellar and relatively dense, which extended to the periphery and transformed into a network structure, and then transformed into rod trabecular bone. The rod-shaped trabeculae converged with the plate-shaped trabeculae with only 1 to 2 layers surrounding the trabeculae cavity. Because rod-shaped trabeculae act as load bearing supports, forces are transferred between the plate trabeculae parallel to the bone cortex and the plate trabeculae surrounding the cavity. Tears occur first when energy converges and is transferred to the weakest trabeculae. Therefore, the platform trabeculae around the trabeculae cavity are most prone to tears. Energy is transmitted along the torn trabeculae, causing fractures.

In this study, microstructural morphological parameters of the C3 to C7 facet of adult cervical vertebrae on the left and right sides and between different vertebral sequences were measured based on micro-CT observation, so as to evaluate the risk of cervical facet injuries. The volume fraction of the trabecular bone is closely related to bone loading capacity and yields strength, and it is the primary index for evaluating the microstructure of trabecular bone.[11–14] The micro-CT system can calculate the density of the selected 3D ROI, and the trabecular volume fraction can be calculated based on 3D reconstruction of voxels. Yamada et al[15] used high-resolution 3D micro-CT to study the microstructure of the lumbar spine and measure the volume fraction of the bone trabecula. It was found that high-resolution 3D assessment of the normal lumbar spine helped to better clarify the microstructure changes. In the compression failure experiment, trabecular volume fraction was closely correlated with vertebral strength (Pearson correlation coefficient, $R^2 = 0.69$), but had a low correlation with trabecular thickness ($R^2 = 0.24$). The bone volume fraction of the ROI predicts the maximum and final stress of the bone. Other studies on spinal micro-CT showed that different ROIs had different microstructures, and the regions with lower volume fraction of bone trabecular bone had lower structural stress, which was the weak area of the vertebral structure.[16] In this study, we measured the differences in the microstructures of C3 to C7 articular processes with different vertebrae sequences. It was found that the volume fraction of the trabecular bone in C7 was significantly different from that in C3 to C6, and the value of trabecular bone volume fraction in C7 was the lowest, indicating that the bone was relatively loose. The bone surface area/bone volume and bone surface density were the lowest at C3 and C4 and C4, with C7 being the highest; however, the overall trend for the trabecular bone volume fraction was the opposite. When the trabecular bone had a constant surface area and trabecular bone volume, the greater the bone trabecular bone area bone volume, the smaller the volume fraction, and this conforms to the experimental parameter change rules of the microstructure. Bone trabecular mode factor is a parameter of bone trabecular connectivity, and the larger the value, the worse the bone trabecular connectivity. In this study, the C7 value was the largest, indicating that C7 has a poor load capacity and is more prone to osteoporosis, fracture, and other diseases.

Previous studies have shown that the microstructure of the articular process is not only related to the shape and stress but is also related to blood flow and distribution of cervical blood vessels. The vertebral artery passes through the transverse foramen of the transverse process of C6 to C1 upward. Due to the small size of the transverse foramen of the C7, only small vertebral veins flow back into it, and the blood supply of the nutritional articular process is relatively small. It may be one of the reasons the C7 facet bone had the lowest volume fraction.[17–19] This also confirmed that C7 is more prone to osteoporosis and degeneration. Therefore, more attention should be paid to blood supply conditions in the clinical evaluation and diagnosis of cervical facet-related diseases, which may have a causal relationship with the functional degeneration of the facet, injury instability, and the resulting abnormal changes in structure and stress balance, and cervical disc degeneration.

In conclusion, micro-CT imaging clearly showed the cervical joints and internal trabecular bone microstructure characteristics and the ossification centers, verifying that the strength of joints and stress degeneration are closely related to the structure of the trabecular bone. This helped to assess the risk of cervical articular injury and provide further evidence regarding the mechanics of changes in the articular process microstructure.

Acknowledgments

We thank Suzhou Haysfield Information Technology Co., Ltd. for providing the specimen scanning and data analysis for this study. We also would like to thank Editage (www.editage.cn) for the English language editing.

Author contributions

Conceptualization: Zhijun Li.
Data curation: Haoyu Song, Peng Wang, Chunying Ma, Yansong Zhang, Yexing Dang.
Formal analysis: Jun Shi, Shaojie Zhang.
Supervision: Xing Wang.
Validation: Yuan Ma.
Writing – original draft: Kun Li.
Writing – review & editing: Yucheng Ji.

References

[1] Manchikanti L, Kosanovic R, Cash KA, et al. Assessment of prevalence of cervical facet joint pain with diagnostic cervical medial branch blocks: analysis based on chronic pain model. Pain Phys. 2020;23:531–40.
[2] Wang HH, Wang K, Deng Z, et al. Effects of facet joint degeneration on stress alterations in cervical spine C_5-C_6: a finite element analysis. Math Biosci Eng. 2019;16:7447–57.
[3] Lee SH, Son DW, Lee JS, Sung SK, Lee SW, Song GS. Relationship between endplate defects, modic change, facet joint degeneration, and disc degeneration of cervical spine. Neurospine. 2020;17:443–52.
[4] Bouxsein ML, Boyd SK, Christiansen BA, Guldberg RE, Jepsen KJ, Müller R. Guidelines for assessment of bone microstructure in rodents using micro-computed tomography. J Bone Miner Res. 2010;25:1468–86.

[5] Ritman EL. Current status of developments and applications of micro-CT. Annu Rev Biomed Eng. 2011;13:531–52.
[6] Perilli E, Parkinson IH, Reynolds KJ. Micro-CT examination of human bone: from biopsies towards the entire organ. Ann Ist Super Sanita. 2012;48:75–82.
[7] Tassani S, Perilli E. On local micro-architecture analysis of trabecular bone in three dimensions. Int Orthop. 2013;37:1645–6.
[8] Zhang ZM, Li ZC, Jiang LS, Jiang SD, Dai LY. Micro-CT and mechanical evaluation of subchondral trabecular bone structure between postmenopausal women with osteoarthritis and osteo porosis. Osteoporos Int. 2010;21:1383–90.
[9] Xiao ZF, He JB, Su GY, et al. Osteoporosis of the vertebra and osteo chondral remodeling of the endplate causes intervertebral disc degeneration in ovariectomized mice. Arthritis Res Ther. 2018;20:1–15.
[10] Denis F. The three column spine and its significance in the classification of acute thoracolumbar spinal injuries. Spine. 1983;8:817–31.
[11] Barrett JM, Mckinnon C, Callaghan JP. Cervical spine joint loading with neck flexion. Ergonomics. 2020;63:101–8.
[12] Rieger R, Auregan JC, Hoc T. Micro-finite-element method to assess elastic properties of trabecular bone at micro- and macroscopic level. Morphologie. 2018;102:12–20.
[13] Liu XS, Sajda P, Saha PK, Wehrli FW, Guo XE. Quantification of the roles of trabecular microarchitecture and trabecular type in determining the elastic modulus of human trabecular bone. J Bone Miner Res. 2006;21:1608–17.
[14] Liu XS, Stein EM, Zhou B, et al. Individual trabecula segmentation (ITS)-based morphological analyses and microfinite element analysis of HR-pQCT images discriminate postmenopausal fragility fractures independent of DXA measurements. J Bone Miner Res. 2012;27:263–72.
[15] Yamada S, Chiba K, Okazaki N, et al. Correlation between vertebral bone microstructure and estimated strength in elderly women: an ex-vivo HR-pQCT study of cadaveric spine. Bone. 2019;120:459–64.
[16] Perilli E, Parkinson IH, Truong LH, Chong KC, Fazzalari NL, Osti OL. Modic (endplate) changes in the lumbar spine: bone micro-architecture and remodelling. Eur Spine J. 2015;24:1926–34.
[17] Li S, Wang C, Shan Z, et al. Trabecular microstructure and damage affect cement leakage from the basivertebral foramen during vertebral augmentation. Spine. 2017;42:E939–48.
[18] Reina N, Cavaignac E, Pailhé R, et al. BMI-related microstructural changes in the tibial subchondral trabecular bone of patients with knee osteoarthritis. J Orthop Res. 2017;35:1653–60.
[19] Greenwood C, Clement JG, Dicken AJ, et al. The micro-architecture of human cancellous bone from fracture neck of femur patients in relation to the structural integrity and fracture toughness of the tissue. Bone Rep. 2015;3:67–75.